Mixing intensification with soft-elastic baffle (SEB) in a soft-elastic reactor (SER)

Minghui Liu, Guangda Zhang, Jie Xiao, Romain Jeantet, Guillaume Delaplace, Yong Wang, Zhizhong Dong, Xiao Dong Chen

Chemical Engineering & Processing: Process Intensification xxx (xxxx) xxx

Contents lists available at ScienceDirect

Chemical Engineering and Processing - Process Intensification

journal homepage: www.elsevier.com/locate/cep

Mixing intensification with soft-elastic baffle (SEB) in a soft-elastic reactor (SER)

Minghui Liu [a,b,#], Guangda Zhang [a,#], Jie Xiao [a,*], Romain Jeantet [c], Guillaume Delaplace [d], Yong Wang [e], Zhizhong Dong [e], Xiao Dong Chen [a,*]

[a] Life Quality Engineering Interest Group, School of Chemical and Environmental Engineering, College of Chemistry, Chemical Engineering and Materials Science, Soochow University, Suzhou, Jiangsu Province 215123, P.R. China
[b] The College of Chemistry and Chemical Engineering, Zhengzhou Normal University, Zhengzhou, Henan Province 450044, P.R. China
[c] STLO, INRAE, Institut Agro, 35042 Rennes, France
[d] UMET - Unité Matériaux et Transformations, UMR 8207 (Univ. Lille, CNRS, INRAE, Centrale Lille), F-59000 Lille, France
[e] Beijing Key Laboratory of Nutrition & Health and Food Safety, COFCO Nutrition & Health Research Institute, COFCO, Beijing 102209, China

ARTICLE INFO

Keywords:
Soft-elastic reactor (SER)
Soft-elastic baffle (SEB)
Flow Visualization
Image analysis
Mixing time

ABSTRACT

Soft-elastic reactor (SER) has been demonstrated as an alternative approach to effective mixing of viscous liquid. Here, the mixing performance of Newtonian fluid—glycerin water solutions (1200±50 mPa·s) was experimentally investigated for the first time inside a simple cylindrical SER with soft-elastic baffle (SEB) aligned in parallel to the SER axis. Visualization based on an acid-base reaction was used to reveal the presence and the disappearance of isolated mixing regions. The mixing performance was characterized using the mixing curve and the mixing time. The effect of SEB positioning on mixing intensification was explored. Results show that a single SEB could improve mixing efficiency with the optimal positioning angle of 90° With the increase of the number of the SEBs, the mixing efficiency was found to be improved regardless of positioning angles. Compared with the SER without SEB, adding a single SEB could reduce the mixing time by about 34% at the probe penetration depth of 2.5 cm and the penetration frequency of 1.0 Hz. Efficient mixing for SERs of large length to diameter ratios was also achieved with the presence of SEB.

1. Introduction

Mixing is a crutial unit operation in chemical engineering and material processing practices such as leaching, polymerization, and cell culturing [1]. In industry, substances in reactors may achieve mixing by resorting to stirrers, oscillatory flows etc. [2–4] and special mixers such as rotor-stators may be needed for processing some highly-viscous fluids [5,6]. The reactor walls are conventionally made by rigid materials. The reactors in nature (e.g. the gastric domains of animals and human) are, however, of soft-elastic materials [7]. The gastric domain, like stomach, can be seen as a reactor, in which the chyme has a viscosity of about 1Pa·s [8]. Inside stomach, different meal components and gastric secretions (i.e. usually solids and liquids) co-exist [9]. The mixing inside gastric track is induced by wall deformation (compression, segmentation contraction and peristalsis) [10]. In recent years, peristalsis of the gastric wall has been applied to the design of in vitro gastric devices for food digestion investigation, including a human gastric simulator (HGS) [11], a human gastric digestion simulator (GDS) [12], and an in vitro mechanical gastric system (IMGS) [13]. The mixing performance of a human gastric digestion simulator (c_GDS) was characterized using a tracer method [14]. The containers of these devices are made of soft materials (e.g. silicon rubber) and the wall deformation induces the flow and hence fluid mixing. The contributions of wall deformation on mass transfer and mixing were confirmed. In a previous work carried out by the same team, the residence time distribution (RTD) in a SER tubular device (inspired by the small intestine of human), was studied [15]. The degree of starch hydrolysis inside the SER tube was measured and compared with that in a stirred rigid tank. The SER can offer better performance compared with the stirred tank under equivalent conditions [16]. In a recent work, to compare more directly with the mixing performance of the stirred rigid tank, a cylindrical SER was made, whose wall was pushed to deform by a rectangular probe periodically [17,18]. The results showed that the mixing time of the SER was shorter than the

* Corresponding authors.
E-mail addresses: jie.xiao@suda.edu.cn (J. Xiao), xdchen@mail.suda.edu.cn (X.D. Chen).
# The first two authors contributed equally to this work

https://doi.org/10.1016/j.cep.2021.108764
Received 27 September 2021; Received in revised form 5 December 2021; Accepted 12 December 2021
Available online 16 December 2021

Nomenclature

a	baffle width (cm)
b	baffle width (cm)
c	baffle thickness (cm)
d	wall thickness (cm)
h	baffle off-bottom clearance (cm)
H	liquid level height (cm)
H_1	total height of the soft elastic reactor (cm)
H_2	the distance between the SER bottom and the base of the SER (cm); or the thickness of the bottom of the SER
M%	mixing degree (%)
$N_{MixedPixels}$	number of mixed pixels (dimensionless)
$N_{TotalPixels}$	number of total pixels (dimensionless)
D_1	external diameter of the SER (cm)
D_2	inner diameter of the SER (cm)
t	time (s)
t_m	mixing time (s)
X	pixel separation value (%)

Greek letters

β	threshold used on a RGB component for color separation (dimensionless)
θ	penetration angle (dimensionless)

team is made of silicone rubber with good biocompatibility, which may be applied to general biotech field, including the mixing of the shear-sensitive cells and the microbial fermentation [20,21]. Other materials with soft-elastic characteristics (e.g. fluoride rubber) had also been attempted, which may be applied to the cases requiring antioxidant and anti-corrosion conditions.

In laminar regime, poor mixing is witnessed by the formation of isolated mixing regions. The isolated mixing regions (IMRs) refer to the localized mixed zones [22]. In order to obtain complete mixing, longer mixing time is usually required [23,24]. Many researchers have made great efforts to eliminate IMRs inside the traditional stirred tanks [25–28]. The mixing efficiency can be improved mainly by inserting baffles, installing off-center impellers, and/or using the inclined impeller, etc. [29–32]. Recently, a silicone flexible section was connected to the blade of the traditional rigid impeller to enhance the mixing efficiency. The disturbance was induced inside the tank with the deformation of the silicone flexible section when the impeller was rotated [33–35]. These studies triggered more ideas for the enhancement of the current SERs. In a previous study in our laboratory, the isolated mixing regions were observed inside the cylindrical SER (without baffle) in the laminar regime [19]. It was expected that the mixing can be improved with the placement of soft-elastic baffles (SEB).

Therefore, in this study, SEB is of the interest. Inside the intestinal tract, the surface villus can enhance the material transfer with the wall peristalsis. The mixing in the small intestine featuring circular folds or villi on the wall surface was investigated by numerical simulation [36, 37]. Inspired by this phenomenon and study, a soft-elastic baffle was

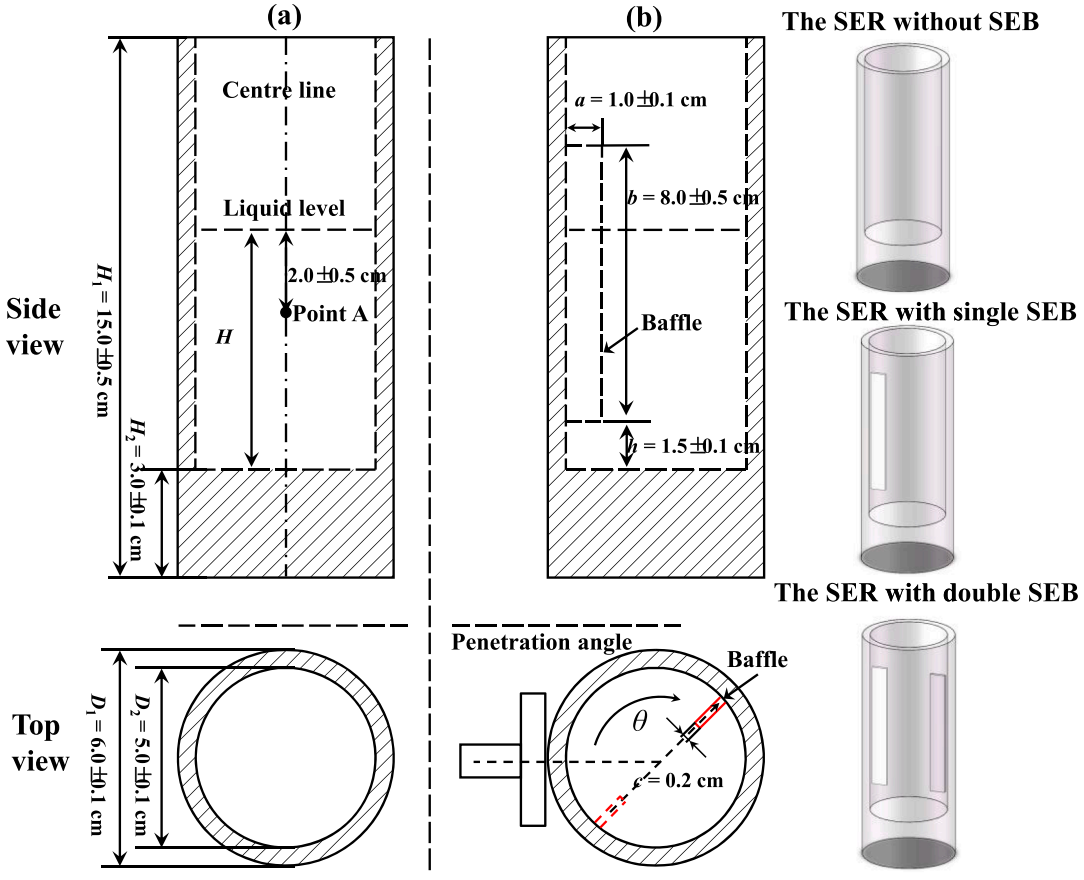

Fig. 1. Schematic diagram of the soft-elastic reactor (a) the unbaffled and (b) the baffled.

rigid stirred tank at low *Reynolds* numbers ranging from 10 to 1000 [19]. These studies suggest that a rational design of SER may be a good alternative for mixing highly viscous materials. The SER used in our fixed on the inner wall surface of the cylindrical SER. It is expected to be able to destroy the circumferential symmetry as far as the mixing is concerned. The soft-elastic fin can deform with the reciprocating

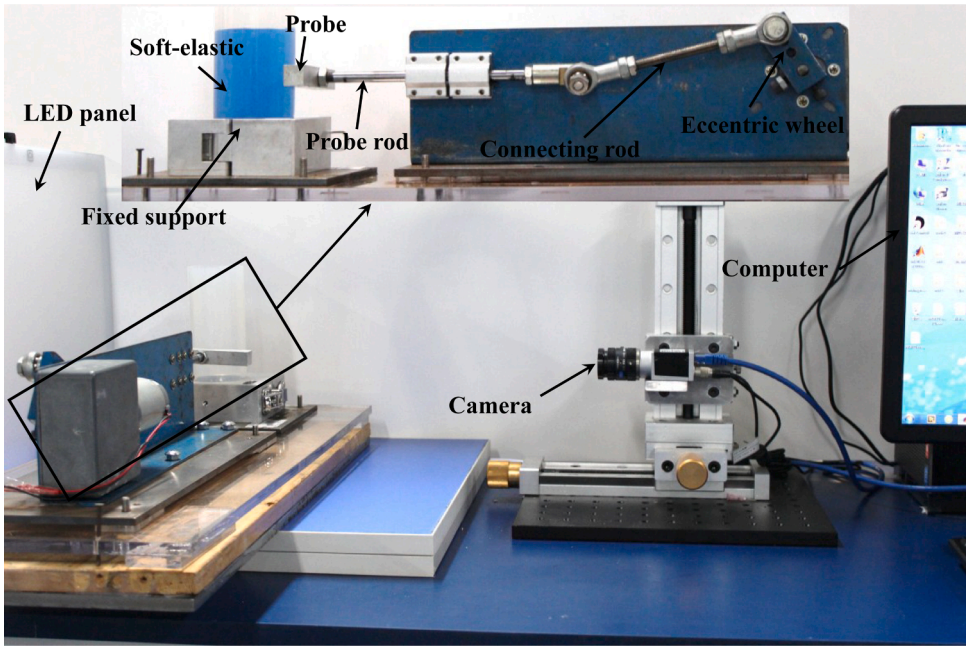

Fig. 2. Schematics shown in the photo of the experimental setup.

impacting (penetration) movement of the probe described in [19], which can induce additional benefits. The mixing performance of the glycerin water solutions (1200±50 mPa·s) (Newtonian) in this baffled SER was investigated, and compared with that of the smooth SER. The effects of the baffle location, the penetration depth and impacting frequency of the probe, the number of the SEBs and the liquid level in the SER on the mixing efficiency were thoroughly studied. The decolorization method based on an acid-base neutralization reaction was used to characterize flow structures. Image analysis was employed to determine the mixing curve (the degree of mixing versus time) and the mixing time. This study has demonstrated the usefulness of the SEB for enhancing the mixing efficiency of SER.

2. Materials and methods

2.1. Experimental setup

The experiments were conducted in two identical soft-elastic reactors: the one that has no baffle and the one that does. The schematics of the baffle-less and the baffled soft-elastic reactors are presented in Fig. 1. These were made in our laboratory.

The height H_1 was 15.0 ± 0.5 cm. The base height H_2 was 3.0 ± 0.1 cm in order to keep the SER fixed well during the impact-penetration process. The external diameter D_1 and the inner diameter D_2 were 6.0 ± 0.1 cm and 5.0 ± 0.1 cm, respectively. The wall thickness d was 0.5 ± 0.1 cm and the wall was made transparent. The baffle had a width a, length b, and thickness c which were 1.0 ± 0.1 cm, 8.0 ± 0.5 cm, and 0.2 cm, respectively. The distance h between the inner bottom and the baffle was 1.5 ± 0.1 cm. The impact-penetration probe was a rectangle. Its dimension was 1.5 cm × 1.5 cm × 10 cm. The liquid level H was maintained at three values, 5.5, 6.5, and 8.0 cm, respectively in different experimental sets. For the SER with one baffle, the angle θ has been defined as the angle between the baffle and the vertical plane cut through the centerline of the impact-penetration probe (Fig. 1), including, 0°, 45°, 90°, 135°, and 180° respectively in different experiments. The SERs and the SEBs were made by using the double component silicon rubber. The method of making SER has been depicted in our previous study [15,17]. The schematic diagram of the experimental set-up is shown in Fig. 2.

The fluid mixing was triggered by an impact-penetration probe devised through the connecting rod and the reciprocating probe. The reciprocating motion of the probe was activated and powered by a DC motor via the connecting rod. In the current work, two parameters, i.e., the impact-penetration depth and frequency, are defined, corresponding to the maximum wall deformation depth (cm) of the SER and the number of impacts per second (s), respectively, as shown in Fig. 3. The impact-penetration location is defined as the distance between the central line of the penetration probe and the bottom of the SER, which was kept constant at 2.5 cm in all experiments.

For the image capturing system, it consisted of an LED panel, a CMOS camera and a computer. To reduce the background noise, an LED panel was also placed behind the SER. The decolorization process of fluid mixing was recorded using a CCD camera (acA1600–60 gc, Germany) linked to a computer.

2.2. Working fluid

The glycerin water solutions were used as the model fluid in all the experiments. The viscosity (about 1200±50 mPa·s) of the glycerin solution was measured at 23 °C by a Brookfield Viscometer (DV-11+Pro, USA). It is necessary to mention that the viscosity of the glycerin solution is sensitive to temperature changes. The environmental temperature was kept at 23 °C with an air-conditioning system.

2.3. Measurement of mixing time

2.3.1. Decolorization reaction

The decolorization reaction has been widely used for visualizing the mixing process [38]. A fast acid-base indicator reaction (Bromothymol blue, 0.01%w/w in a mixture of water and alcohol) was used. The indicator is yellow when pH ⟨ 6.0 and blue when pH ⟩ 7.6. First, approximately 2.5 mL indicator solution was added into the 500 mL model fluid. Subsequently, 1.5 mL of the 1 mol/L NaOH solution was added. This solution was then mixed until a uniform blue color was observed. The color changes from blue to yellow in all experiments after the addition of acid solution (Fig. 3). It is easier to observe the isolated regions in a yellow liquid [39].

The solution was placed for an hour to remove the gas bubbles before the rotor start-up. The volume of solution in each experiment varies with the height of the liquid surface. Then the 1 mol/L HCl solution (a

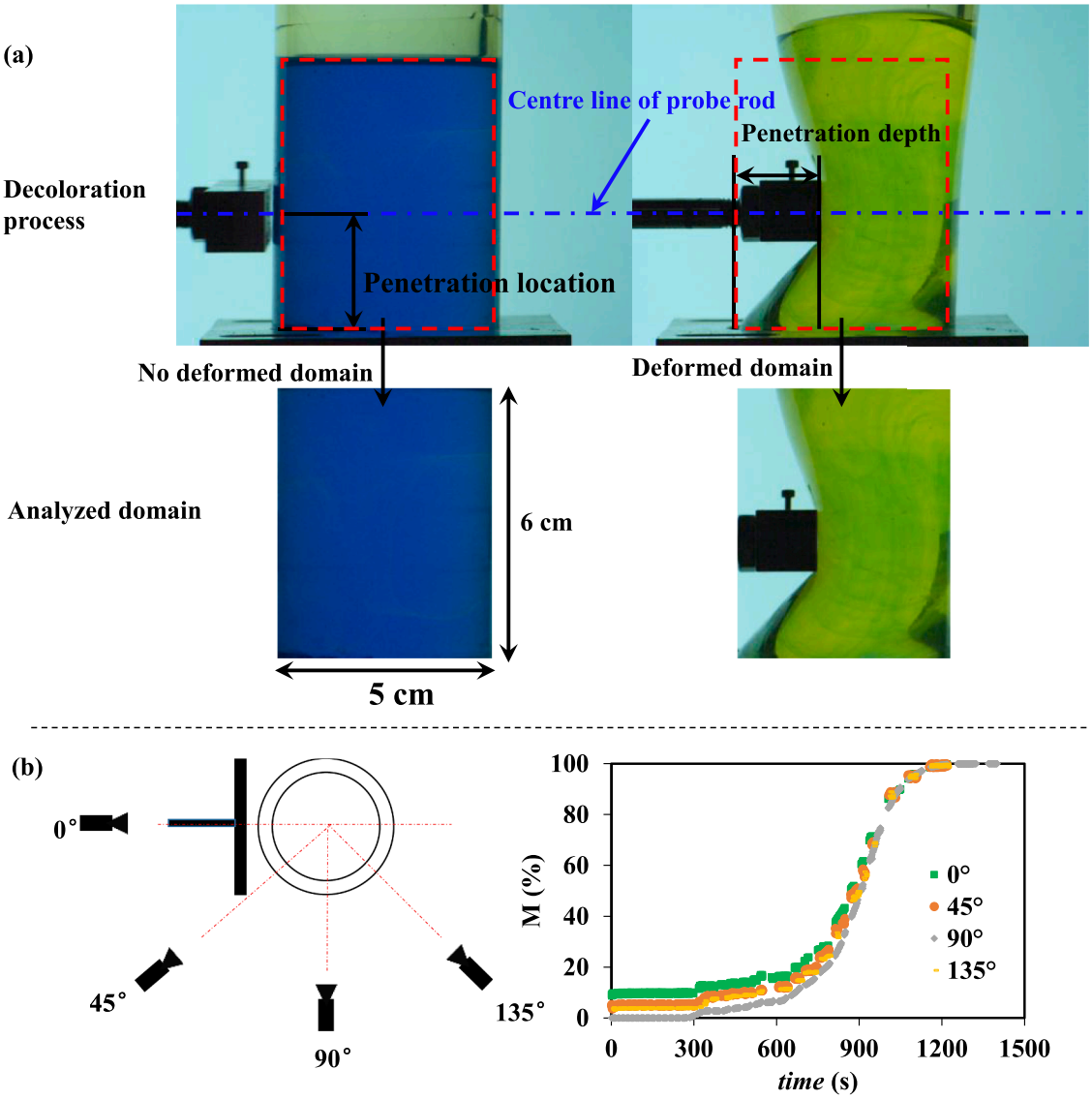

Fig. 3. (a) The decolourization process and the domain of the visualization images. (b) The relative position of equipment and camera and the mixing curve under different angle (non-baffle, frequency 1hz, penetration depth 2.5 cm).

mixture of acid, water and glycerin, which had a viscosity close to the bulk solution) was rapidly injected into the bulk solution at a location of 2 ± 0.5 cm below the liquid level. The ratio of acid-to-base is approximately equal to 2.0, minimizing the influence of chromatic aberration on the results. The visualization images of the decolorization process varying from blue to yellow, was stored (TIFF format) at a recording frequency of 1.00 Hz.

2.3.2. Image analysis

The decolorization reaction can be used to measure mixing time [40]. In this work, based on the RGB color model, the RGB based image analysis method proposed by Cabaret et al. was used to measure the mixing time [41]. The RGB color model consists of three channels, i.e., R (red), G (green), and B (blue) channels. For the indicator Bromothymol blue used in this work, the single channel R was used in order to save the computational resource [42]. The local threshold β can be defined using the equation: $\beta = R_0 + (R_0 - R_\infty) \times 50\%$, where R_0 and R_∞ are respectively the average value of R channel of all pixels in the five initial images (before mixing) and the five images of the finally mixed. When $R_{ij} \geq \beta$, the pixel (i, j) was defined as a pixel of the mixed, when $R_{ij} < \beta$, the pixel (i, j) was defined as a pixel of the unmixed. The number of the mixed pixels $N_{\text{Mixed Pixels}}$ at any instant t was counted when the value of red channel of a single pixel became larger than the local threshold β. The degree of mixing M% ($N_{\text{MixedPixels}}/N_{\text{TotalPixels}}$) was plotted against time t to obtain the mixing curve. The mixing time t_m was determined when the degree of mixing was 95%. For all the experiments, only the images when the reactor came back to the undeformed positions were analyzed (see Fig. 3a). It should be noted that each experiment was repeated three times and average values were calculated for analysis. Although the mixing curves based on data taken from different viewing angles were slightly different during the initial stage of mixing, the mixing curves for the final stage of mixing overlap. Viewing angles did not affect mixing time as well (see Fig. 3b).

2.3.3. Generation of the map of the local mixing time

The distribution of local mixing time for each pixel in the reactor domain is very important information [43,44]. The local mixing time, which is a good indicator for the local mixing efficiency, was evaluated as follows. A threshold value β was first specified. At time t, the red channel values of all pixels which had not been assigned a mixing time value in the image were compared with this threshold value β. The pixels having a red channel value bigger than β were assigned a local mixing

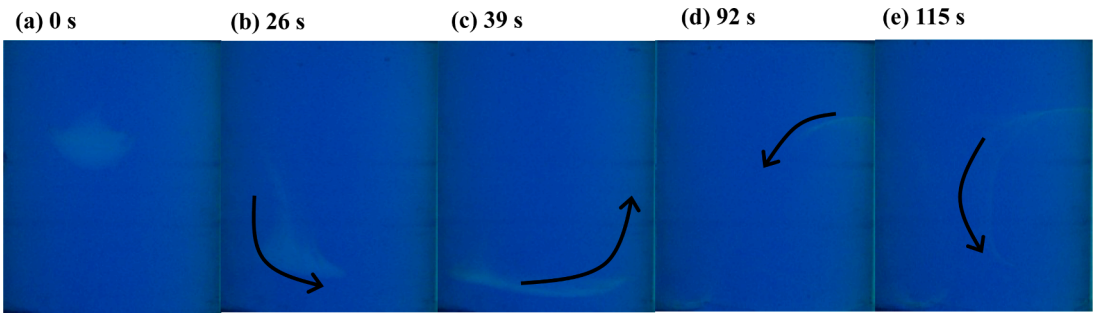

Fig. 4. The streak lines on the initial stage of an acid blob (injected at one point) are stretched inside the unbaffled SER. The lines indicate that the directions of material being stretched and folded.

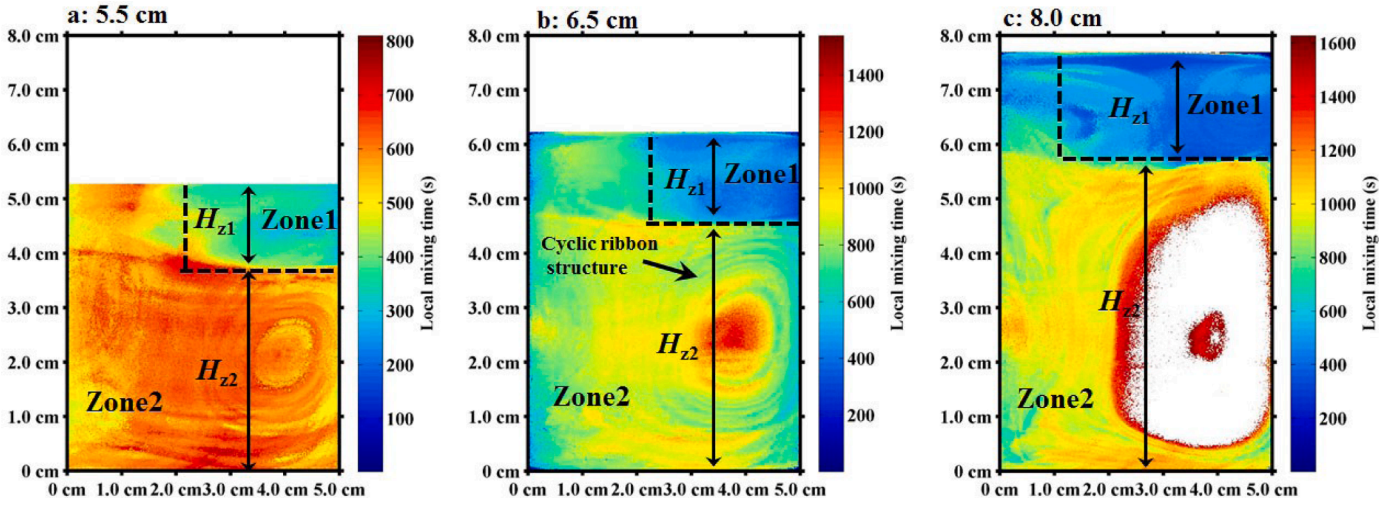

Fig. 5. The local mixing time maps reconstructed from the mixing process of the unbaffled SER at three liquid levels. (a) 5.5 cm, (b) 6.5 cm and (c) 8.0 cm respectively. The color bar on the right hand side represents the relationship between color and mixing time. the white color indicates the mixing time could not be obtained. The penetration frequency was 1.00 Hz.

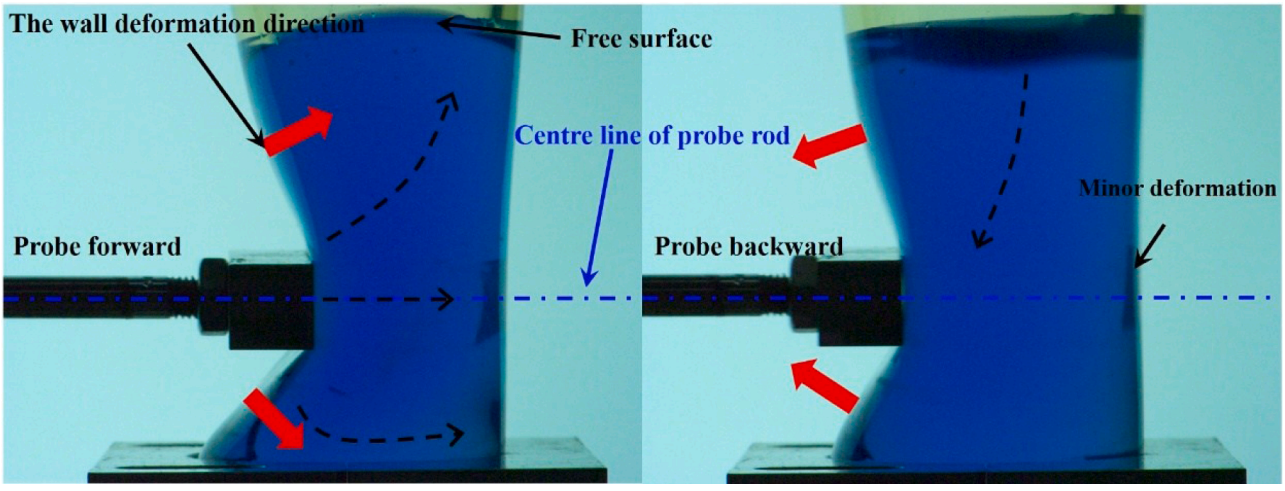

Fig. 6. The sketch of fluid flow direction inside soft-elastic reactor for two stages, forward and backward. The red arrow indicates the direction of wall deformation.

time value of t. Once a pixel got a mixing time value, this value was kept unchanged for this pixel. All images taken at different times during one experiment were processed in this way to generate one distribution map of the mixing time. It must be noted that the red channel value of a pixel in the isolated region is always smaller than the local threshold β, the local mixing time thus could not be obtained. As such, the local mixing time of a pixel at the isolated region was not plotted.

3. Results and discussions

3.1. Analysis of the flow patterns in the unbaffled SER

In order to better understand the mixing performance, the mixing pattern of the unbaffled and baffled SER should be investigated. The stretching and folding of the material elements are usually thought to be

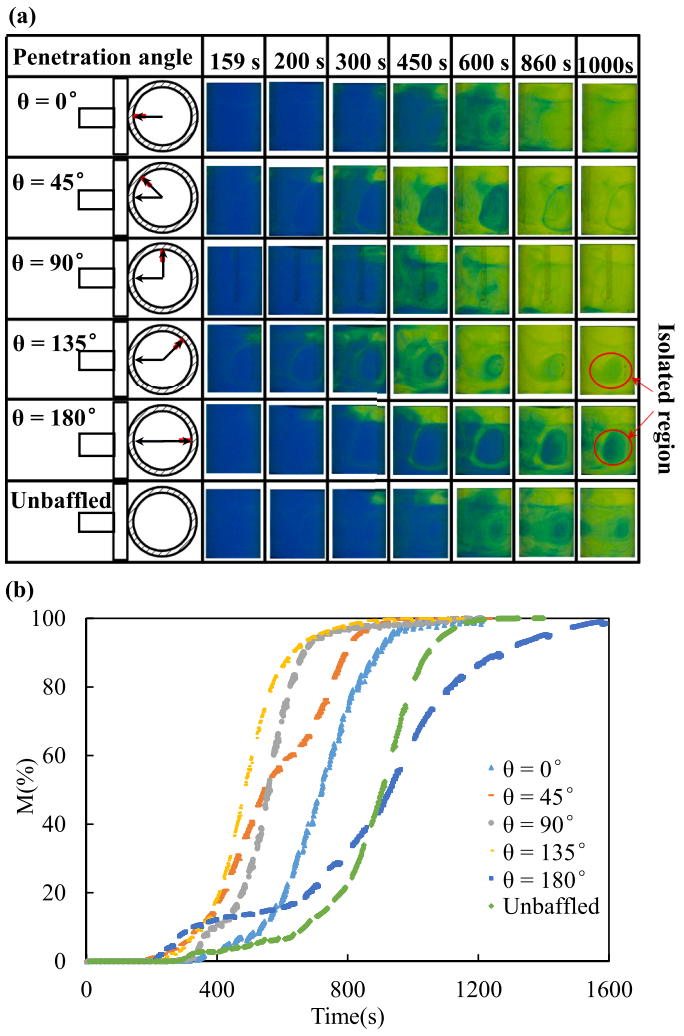

Fig. 7. (a) Visualization images and (b) Mixing curves for the SER with SEB at different penetration angles and without SEB at penetration frequency of 1.00 Hz.

the main mixing pattern for the highly viscous fluid [45]. The pattern of the streak lines stretched and folded inside the unbaffled soft-elastic reactor is shown qualitatively in Fig. 4. Although the streak lines depicted in the images are based on the 2-D plane from the viewing angle of the researcher, which may have some differences from the actual movement of the acid solutions injected inside the 3D reactor, the stretching and folding were obvious. The experiments were conducted at the impact-penetration frequency of 1.00 Hz, the penetration depth of 2.5 cm and the penetration location of 2.5 cm. The acid solution was injected at 2.0 ± 0.5 cm depth below the liquid surface.

First, the streak lines were stretched towards the lower section from the injection position, the streak lines were then stretched horizontally along the bottom to the right corner, as shown in Fig. 4b. Subsequently, the streak lines were stretched upwards, as shown in Fig. 4c. The streak lines finally returned to the right corner of the bottom, shown in Fig. 4d and 4e. A more comprehensive understanding of the mixing dynamics can be obtained from the local mixing maps. Fig. 5 shows the local mixing maps reconstructed from the mixing process of unbaffled SER at three liquid levels.

It can be seen from Fig. 5 that Zone 1 and Zone 2 are obviously different in color corresponding to their local mixing times for different liquid levels. It indicates that the mixing patterns at Zone 1 and Zone 2 are different from each other. In Zone 1, the mixing time was shorter than the mixing time at Zone 2. The velocity gradient was enhanced due

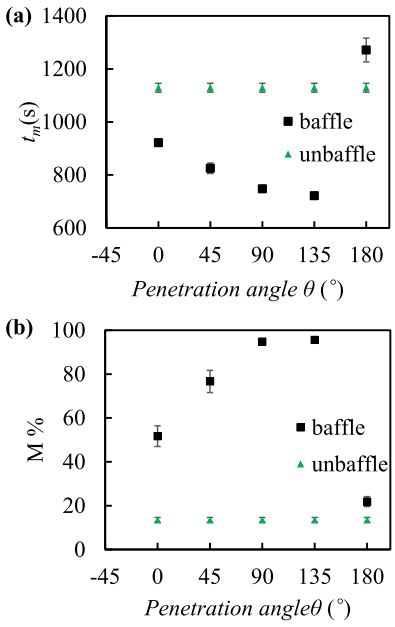

Fig. 8. (a) The mixing time at different penetration angles for the SERs with SEB and without SEB; (b) Comparison of the mixing degree which was obtained at the time t equal to tm for the penetration angle 90° The penetration frequency was 1.00 Hz.

to the moving free surface formed during the reciprocating penetration process (Fig. 6) [46].The greater the velocity gradient, the shorter the mixing time. With the increase of the liquid levels, the H_{z1} of Zone 1 has not changed. At Zone 2, a kind of cyclic ribbon structure was observed. The process of stretching and folding of the streak lines was the dominant mixing mechanism (Fig. 4). With the increase of the liquid levels, compared with the H_{z1}, the H_{z2} of Zone 2 was obviously increased. It indicated that when the liquid level was increased, the axial stretched distance was increased.

In order to better understand the stretching and folding in Zone 2, Fig. 6 shows a sketch of fluid flow direction. The forward and backward movement of the probe is a kind of reciprocating penetration process. During the forward movement, the fluid flows along the same direction and upward following the wall deformation. It has resulted in the fluid stretching and folding along the same direction, as shown in Fig. 4b and 4c. The fluid flow direction inside the unbaffled soft-elastic reactor is more conformed to the wall deformation angle. The obvious difference of wall deformation angles was observed at the upper and lower regions relative to the centerline of penetration rod. It has resulted in two different fluid flow directions respectively exist in the upper and lower regions. During the backward movement, the fluid flows following the retrieving probe and downward with the restoration of the wall. It leads to the fluid elements to be stretched and folded as shown in Fig. 4d and 4e.

For the baffled SER, the mixing pattern was affected also by the deformation of the soft baffle. The mixing performance of the SER with SEB has been compared using the visualization images and the mixing curves to be described in the next section.

3.2. *Effect of penetration angle on the mixing performance*

In the current work, a soft-elastic baffle (SEB) was vertically fixed onto the inner wall of the SER (refer to Fig. 1). The SEB can also be deformed, triggered by the action of the impact-penetration probe. The fluid could then be disturbed by deformation of the soft-elastic baffle. The effect of the penetration angles on the mixing performance was thoroughly studied. At the same time, the enhancing effect of penetration angle on mixing performance was studied under different

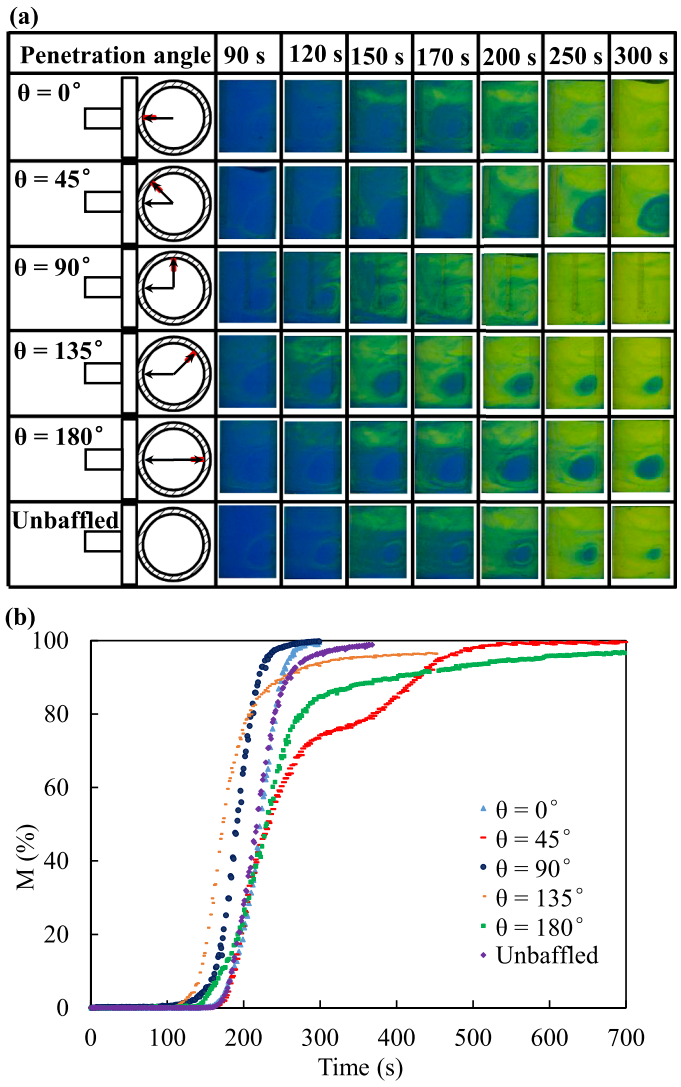

Fig. 9. (a) Visualization images and (b) Mixing curves for the SER with SEB at different penetration angles and without SEB at penetration frequency of 1.67 Hz.

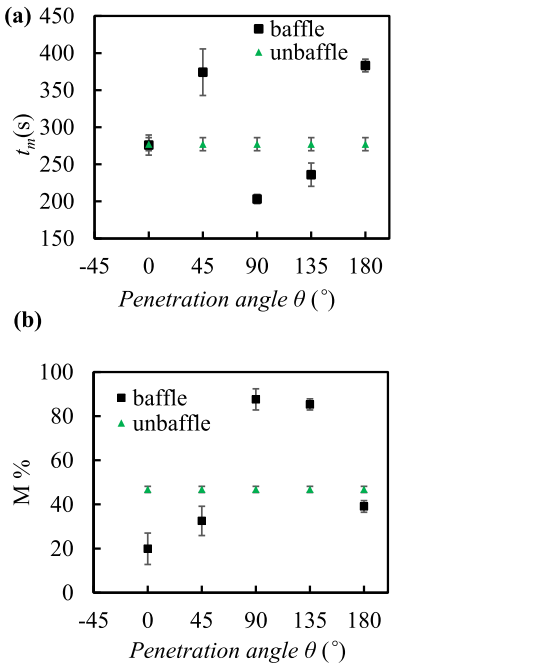

Fig. 10. (a) The mixing time at different penetration angles for the SERs with SEB and without SEB; (b) Comparison of the degree of mixing which was obtained at the time t equal to tm for the penetration angle 90° The penetration frequency was 1.67 Hz.

penetration frequencies and depths.

3.2.1. Effect of impact-penetration frequency

The isolated regions and the evolution of the degree of mixing were analyzed using the images and the mixing curves. Five impact-penetration angles were selected including 0°, 45°, 90°, 135°, and 180° respectively. In all the experiments, the penetration depth and location were both kept at 2.5 cm, the liquid level (liquid height) was maintained at 6.5 cm.

All experiments were conducted at two impact-penetration frequencies 1.00 and 1.67 Hz, respectively. Fig. 7a shows the visualization images at the penetration frequency of 1.00 Hz. It can be seen that the penetration angles have an obvious influence on the structure of the isolated regions. At the penetration angles of 0° and 90°, the poor mixing regions cannot be observed. In the initial stage of the mixing, the poorly mixed regions can be observed at the penetration angles of 45 °, 135° and 180°, respectively, and the size of the isolated region inside the SER with SEB was larger than that inside the unbaffled SER. At a later stage, the regions became mixed at the penetration angles of 45 ° and 135° Fig. 7b shows the mixing curves obtained at different penetration angles. It can be seen that the mixing efficiency was enhanced at the penetration angles of 0°, 45°, 90°, and 135° compared with the unbaffled SER, even the isolated regions was observed inside the SER with SEB at the penetration angles of 45° and 135° For penetration angle of 180°, the degree of mixing of the SER with SEB was higher than the degree of mixing of the unbaffled at the earlier stage. It is because perhaps in addition to the basic SER effect, the deformation process of the soft-elastic baffle and the dynamics of the free surface combined had enhanced the mixing efficiency at this stage. However, the degree of mixing of the SER with SEB was lower than the mixing degree of the unbaffled SER at the later stage due to the formation of larger isolated regions (see the circled region in Fig. 7(a)).

For quantitative analysis, the mixing time and the degree of mixing are shown in Fig. 8. The mixing time of the SER with SEB was lower than the mixing time of the unbaffled SER. The results indicate that the soft-elastic baffle can promote the mixing efficiency. At the penetration angles of 90° and 135°, the mixing time of the SER with SEB was reduced by 33.8 ± 1.5% compared with the unbaffled SER (Fig. 8a) and the degree of mixing of the SER with SEB was about 7 times larger than that for the unbaffled SER (Fig. 8b). At the penetration angle of 90°, the maximum deformation was obtained compared with other penetration angles, which led to the maximum disturbance. The higher the disturbance to the liquid mixing, the more obvious the reduction in the mixing time.

The analysis of the experiments at penetration frequency of 1.67 Hz was similar to the penetration frequency of 1.00 Hz. It can be seen from Fig. 9(a) that the isolated regions could not be observed at the penetration angles of 0° and 90° during the whole mixing process, and the isolated regions appeared at the penetration angles of 45°, 135° and 180° Furthermore, the size of the isolated region inside the SER with SEB at the penetration angles of 45°, 135° and 180° was larger than the size of the isolated region inside the unbaffled SER. The results at the penetration frequency of 1.67 Hz were similar to the results at penetration frequency of 1.00 Hz. Fig. 9b shows the mixing curves obtained at different penetration angles. Compared with the unbaffled SER, the mixing efficiency (evaluated by the mixing time and mixing degree in this work) at the penetration angles of 90° and 135° was significantly improved. However, due to the formation of the isolated region, the

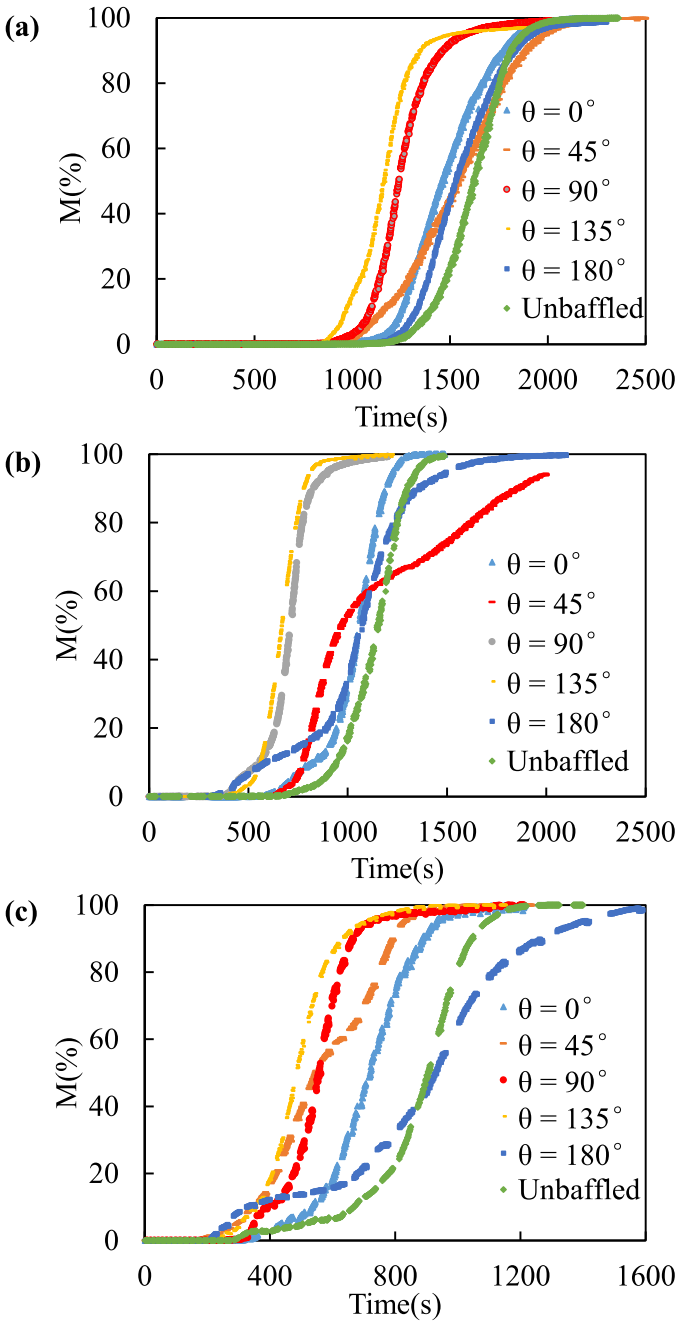

Fig. 11. The mixing curves of the SER with SEB at different penetration angles and without SEB at different penetration depths. (a) 1.5 cm; (b) 2.0 cm; (c) 2.5 cm. The penetration frequency was 1.00 Hz.

complete mixing could not be achieved at the penetration angle of 135°. At the penetration angles of 0°, 45°, and 180°, the mixing efficiency was similar to the unbaffled SER at the earlier stage. Differences were observed due to different structures of the isolated regions at the later stage according to the visualization images (Fig. 9a).

Fig. 10a shows the mixing time of the SERs with SEB and without SEB. At penetration angles of 45° and 180°, the mixing time of the SER with SEB was slightly longer than the mixing time of the unbaffled SER. At the penetration angles of 0° and 135°, the mixing time of the SER with SEB was almost equal to the mixing time of the unbaffled SER. Only at the penetration angles of 90°, the mixing time of the SER with SEB was reduced by 22.8 ± 1.6% compared with the unbaffled SER, and the degree of mixing of the SER with SEB was about 1.8 times higher than the mixing degree of the unbaffled SER (Fig. 10b). However, there is no

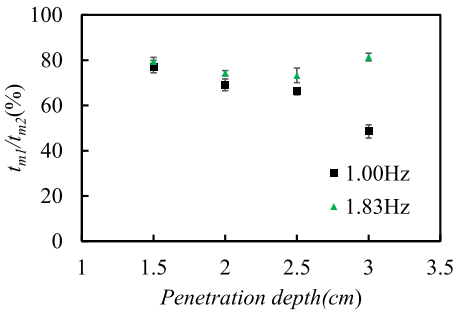

Fig. 12. The ratio (tm1/tm2) variation against the penetration depth, at the penetration frequencies of 1.00 and 1.83 Hz respectively. The penetration angle was 90°

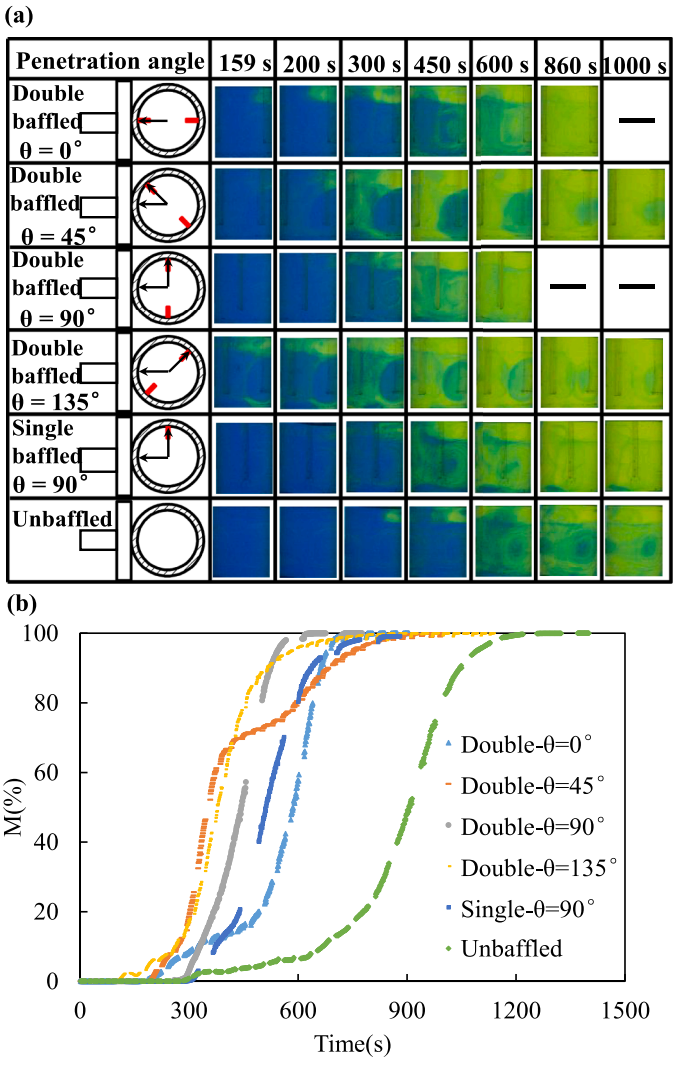

Fig. 13. (a) Visualization images and (b) Mixing curves for the SER with double SEBs, the SER with single SEB, and the unbaffled SER at the penetration frequency of 1.00 Hz.

doubt that the soft-elastic baffle vertically fixed to the wall of the unbaffled SER is able to improve mixing efficiency at the penetration angle of 90° judged by the behaviors of the isolated regions and mixing times.

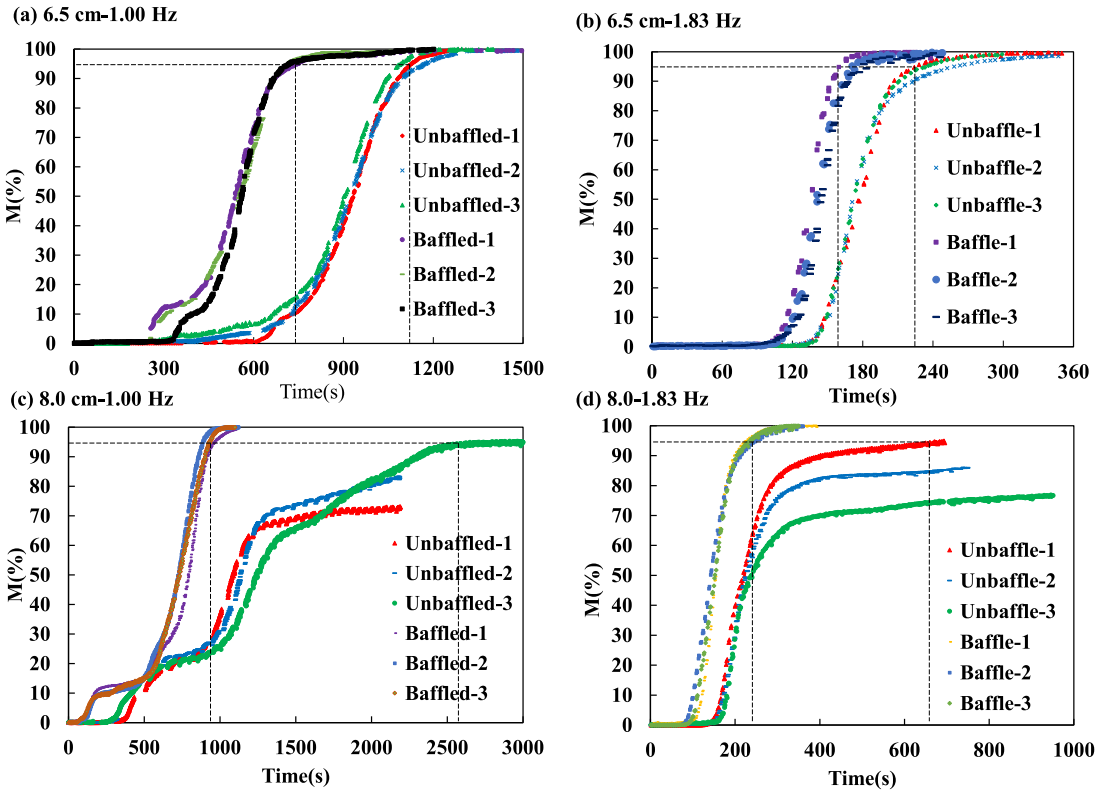

Fig. 14. The mixing curve of the baffled and unbaffled SER at different liquid levels. (a): 6.5 cm-1.00 Hz; (b) 6.5 cm-1.83 Hz; (c) 8.0 cm-1.00 Hz; (d) 8.0 cm-1.83 Hz.

Table A1
The mixing time under different experimental conditions.

Frequency (Hz)	Penetration depth (cm)	Baffle	Penetration angle (°)	t_{m95} (s)
1	1.5	–	–	2040
1	2.0	–	–	1281
1	2.5	–	–	1129
1	3.0	–	–	1318
1	1.5	1	90	1574
1	2.0	1	90	885
1	2.5	1	90	747
1	3.0	1	90	639
1	2.5	1	0	921
1	2.5	1	45	825
1	2.5	1	90	747
1	2.5	1	135	721
1	2.5	1	180	1271
1.67	1.5	1	90	453
1.67	2.0	1	90	309
1.67	2.5	1	90	221
1.67	3.0	1	90	136
1.67	2.5	–	–	284
1.67	2.5	1	0	267
1.67	2.5	1	45	433
1.67	2.5	1	90	221
1.67	2.5	1	135	279
1.67	2.5	1	180	514
1.83	1.5	1	90	602
1.83	2.0	1	90	269
1.83	2.5	1	90	170
1.83	3.0	1	90	144
1.83	2.5	–	–	232
1.83	2.5	1	0	194
1.83	2.5	1	45	273
1.83	2.5	1	90	170
1.83	2.5	1	135	196
1.83	2.5	1	180	293

3.2.2. *Effect of penetration depth*

The penetration depth not only affected the maximum deformation of the wall of the soft-elastic reactor, but also the maximum deformation of the soft-elastic baffle. In the present work, the effect of penetration depth on enhancing the performance of the soft-elastic baffle under different penetration angles was analyzed.

Fig. 11 shows the mixing curves of different penetration angles at the penetration depths of 1.5, 2.0, and 2.5 cm. At the penetration angles of 90°and 135°, even at the low penetration depth of 1.5 cm, the mixing efficiency of the SER with SEB was obviously higher than the mixing efficiency of the SER with SEB at other penetration angles and as well, the unbaffled SER. Results indicate that the small disturbance caused by the deformation of the soft-elastic baffle can also enhance the liquid mixing at the penetration angles of 90° and 135° Moreover, the difference between the mixing curves under other penetration angles of 0°, 45°, and 180° becomes more significant with the increase of penetration depth from 1.5 to 2.5 cm. The results indicate that, the enhancement of the soft-elastic baffle under different penetration angles on mixing efficiency was affected by the penetration depth. In pervious section, the best penetration angle is found to be 90°

In order to compare the enhancing effect of the soft-elastic baffle for the penetration angle of 90° under different penetration depths, the ratio of t_{m1}/t_{m2} was calculated, where t_{m1}, t_{m2} is the mixing time of the SER with SEB for the penetration angle of 90° and the unbaffled SER, respectively. The smaller the ratio, the more obvious the enhancing effect of the penetration depth on the mixing efficiency is. Fig. 12 shows that the ratio (t_{m1}/t_{m2}) variation with the penetration depth. At the low penetration frequency of 1.00 Hz, with the increase of penetration depth, the variation of the ratio (t_{m1}/t_{m2}) was more obvious than that at the high penetration frequency of 1.83 Hz. When the penetration depth increased from 1.5 to 3.0 cm, at the low penetration frequency of 1.00 Hz, the ratio (t_{m1}/t_{m2}) was reduced from 77.2 ± 1.6% to 48.5 ± 2.2%. It indicates that when the penetration frequency is low, the enhancing effect of the penetration depth becomes more obvious with the

increasing penetration depth. While at the high penetration frequency of 1.83 Hz, the average ratio (t_{m1}/t_{m2}) was found to be 77.1 ± 1.6%. The enhancing effect may be affected by the penetration depth. The reason is that at the high penetration frequency of 1.83 Hz, the deformation velocity of the liquid inside the SER with the baffle was fast enough so that the improvement of the disturbance by increasing the penetration depth can be neglected.

3.3. Effect of the number of soft-elastic baffles (SEB)

The effect of the number of the soft-elastic baffles on mixing performance was also explored. For the single SEB system, the mixing efficiency of the SER can be enhanced at the impact-penetration angle of 90° The SER with double SEBs was made (Fig. 1 and 13). Two baffles were placed in an asymmetric way. For the SER with double SEBs, the effect of the penetration angle on mixing performance was studied and compared with the SER with a single SEB and no SEB. Fig. 13 shows the visualization images and mixing curves of the mixing processes.

For the SER with two baffles, although the isolated regions could be seen at penetration angles of 45° and 135° at the initial stage of mixing, the isolated regions disappeared at the later stage. At penetration angles of 0° and 90°, the poor mixing regions could not be observed. Results seem similar to the SER with a single SEB. According to the mixing curve, it is anticipated that multiple soft-elastic baffles would further improve the mixing efficiency. The mixing time for the SER with double SEB was shorter than that of the unbaffled SER at all selected penetration angles. The effect of the number of the SEBs on the mixing efficiency was analyzed using the mixing time at different penetration angles (single baffle with $\theta = 90°$ and double baffle with $\theta = 90°$). The mixing time values of the unbaffled SER, the SER with a single SEB and the one with double SEBs were 1129 s, 747 s and 557 s, respectively. Compared with the unbaffled SER, the mixing time values of the SER with a single SEB and double SEBs were shortened by 382 s and 572 s, respectively. It should be noted that when the number of the SEBs increased from one to two, the mixing time was shortened by 190 s, which is lower than the value of 382 s for the single SEB.

3.4. The enhancement effect of SEB under different length-diameter ratios

For a stirred tank reactor, the length-diameter ratio is an important parameter. If the length-diameter ratio is too large, it may cause a series of problems such as longer mixing time or lower degree of mixing. For SER, the enhancement effect of the SEB on mixing performance was also studied under different length-diameter ratios ranging from 1.3 to 1.6. Fig. 14 shows the mixing curves of the SER. It was found that when the length-diameter ratio was 1.3 (i.e., the liquid height of 6.5 cm), the mixing degree could reach more than 95% regardless of whether there is SEB or not. The mixing time could be reduced with the increase of the frequency. Systems with SEBs demonstrated shorter mixing time, i.e., higher mixing efficiency. When the length-diameter ratio was increased to 1.6, the height of liquid became 8 cm. The degree of mixing could still reach 95% or higher in the SER with SEB. However, in the case of unbaffled SER, the degree of mixing was less than 95%, sometimes even less than 70%, and the degree of mixing was not improved effectively with the increase of the frequency. Nevertheless, it can be seen that the addition of soft-elastic baffles not only reduced mixing time, but also achieved efficient mixing under large length-diameter ratios.

4. Conclusions

In this work, the effect of SEB was explored as a means to enhance mixing of the SER. Soft elastic baffle (SEB) was fixed on the wall parallel to the centerline of the same cylindrical SER. The mixing performance was evaluated for a Newtonian fluid (i.e., the glycerin water solutions with a viscosity of 1200±50 mPa·s). The formation of the isolated regions was observed and the mixing time in the SER with and without SEB was evaluated. For the single SEB scenario, the position of the SEB was investigated. For the SER with a single SEB at the impact-penetration angle of 90°, the obvious reduction in mixing time was obtained and the isolated regions were seen to have completely diminished. It was found that the symmetric nature of the fluid flow was destroyed by the deformation of the SEB and the poor mixing regions was diminished. The mixing time was therefore shortened. The number of the SEB on mixing efficiency was explored. When the number of the SEB was increased, the mixing efficiency was enhanced at all impact-penetration angles.

Under the same experimental conditions, when the penetrating frequency is increases, the instantaneous speed of the extrusion head increases at the same time, which leads to the increase of motion speed of the wall impacted by the extrusion head. Since the velocity of liquid adjacent to the opposite wall surface is zero, the velocity gradient in the whole liquid domain increases, which can promote mixing. In addition, the increase of frequency enhances the overall convection in the system, leading to a shorter mixing time. The increase of penetration depth can lead to two consequences: (1) in this specific experimental work, the adjustment of the penetration depth was achieved by increasing the radius of the eccentric, while keeping the frequency the same. Although the angular velocity does not change, the linear velocity of the extrusion head increases with the radius of the eccentric. The movement speed of the wall impacted by the extrusion head increases, which is beneficial for mixing. (2) the amplitude and speed of the wall movement increases with the penetration depth, and the overall convection is then strengthened.

The introduction of the baffle may have the following two influences: (1) the flexible baffle moves with the movement of the flexible wall, which will disturb the fluid flow pattern and facilitate mixing. It was found that when the penetrating angle is 0°, 45°, 90°, or 135°, the mixing time is reduced as compared with the case without baffle. However, when the relative position of the extrusion head and the baffle is 180°, the mixing time increases. It is because the baffle located on the opposite side of the extrusion head can hardly move. When the Reynolds number is low, the baffle will hinder the mixing of nearby fluids. (2) when there is relative movement between the baffle and the fluid, the boundary layer tends to detach from the baffle, leading to vortices near the baffle. When the relative position of the extrusion head and the baffle is 0°, the relative movement is not obvious, but when the relative position of the extrusion head and the baffle is 90°, there is a large relative velocity between the baffle and the fluid, which is the reason for the shortest mixing time when the baffle is at 90° This work has shown that the addition of this soft object is indeed an effective approach to improve the mixing efficiency of the SER. In future, the material strength, width, and height of the soft-elastic baffle can be studied for identifying better SER designs. All these efforts are useful for the exploration of SERs as a potentially effective reactor for certain industrial applications.

Declaration of Competing Interest

None.

Acknowledgments

The authors are grateful for the National Key Research and Development Program of China (International S&T Cooperation Program, ISTCP, 2016YFE0101200), the financial support from the National Natural Science Foundation of China (21676172, 21978184), the Natural Science Foundation of Jiangsu Province (Grants No. BK20170062), and the“Priority Academic Program Development (PAPD) of Jiangsu Higher Education Institutions”. The author XDC came up the idea of SER based on his in vitro digestion studies. He thanks Soochow University for providing the start-up grant for carrying out projects in bio-inspired chemical engineering. Jie Xiao also acknowledges the “Jiangsu

Innovation and Entrepreneurship (Shuang Chuang) Program" and the "Jiangsu Specially-Appointed Professors Program".

Appendix

Table A1

References

[1] E.L. Paul, V.A. Atiemo-Obeng, S.M. Kresta, Handbook of Industrial Mixing: Science and Practice, John Wiley & Sons, Hoboken, 2004.
[2] F. Visscher, J. Van der Schaaf, T.A. Nijhuis, J.C. Schouten, Rotating reactors–a review, Chem. Eng. Res. Des 91 (2013) 1923–1940.
[3] R.K. Thakur, C. Vial, K.D.P. Nigam, E.B. Nauman, G Djelveh, Static mixers in the process industries—A review, Chem. Eng. Res. Des. 81 (2013) 787–826.
[4] A. Mazubert, D.F. Fletcher, M. Poux, J. Aubin, Hydrodynamics and mixing in continuous oscillatory flow reactors—Part I: effect of baffle geometry, Chem. Eng. Process. 108 (2016) 78–92.
[5] V. Vikash, D. Deshawar, V Kumar, Hydrodynamics and mixing characterization in a novel high shear mixer, Chem. Eng. Proces. Process Intensif. 120 (2017) 57–67.
[6] V. Vikash, V. Kumar, Effect of stator geometries on flow fields and mixing performance for viscous fluids, Chem. Eng. Proces. Process Intensif. (2021), https://doi.org/10.1016/j.cep.2021.108595.
[7] X.D. Chen, Scoping biology-inspired chemical engineering, Chin. J. Chem. Eng. 24 (2016) 1–8.
[8] J. Arrieta, J.H. Cartwright, E. Gouillart, N. Piro, O. Piro, Tuval, I.Geometric mixing, peristalsis, and the geometric phase of the stomach, PLoS ONE 7 (2015), e0130735.
[9] B.A. Horwitz, C.A. Blanton, R.B. Mcdonald, Physiologic determinants of the anorexia of aging: insights from animal studies, Food Sci. Technol. 22 (2002) 417–438.
[10] H. Kozu, I. Kobayashi, M. Nakajima, K. Uemura, S. Sato, S Ichikawa, Analysis of flow phenomena in gastric contents induced by human gastric peristalsis using CFD, Food Biophys 5 (2010) 330–336.
[11] F. Kong, R.P Singh, A human gastric simulator (HGS) to study food digestion in human stomach, J. Food Sci. 75 (2010) E627–E635.
[12] H. Kozu, Y. Nakata, M. Nakajima, M.A. Neves, K. Uemura, S. Sato, I. Kobayashi, S. Ichikawa, Development of a human gastric digestion simulator equipped with peristalsis function for the direct observation and analysis of the food digestion process, Food Sci. Technol.Res. 20 (2014) 225–233.
[13] L. Barros, C. Retamal, H. Torres, R.N. Zuniga, E. Troncoso, Development of an in vitro mechanical gastric system (IMGS) with realistic peristalsis to assess lipid digestibility, Food.Res.Int 90 (2016) 216–225.
[14] H. Kozu, I. Kobayashi, M. Nakajima, M.A. Neves, K. Uemura, H. Isoda, S Ichikawa, Mixing characterization of liquid contents in human gastric digestion simulator equipped with gastric secretion and emptying, Biochem. Eng. J 122 (2017) 85–90.
[15] R. Deng, L. Pang, Y. Xu, L. Li, X. Wu, X.D Chen, Investigation on a soft tubular model reactor based on bionics of small intestine–residence time distribution, Int. J. Food. Eng. 10 (2014) 645–655.
[16] R. Deng, C. Selomulya, P. Wu, M.W. Woo, X. Wu, X.D Chen, A soft tubular model reactor based on the bionics of a small intestine–starch hydrolysis, Chem. Eng. Res. Des. 112 (2016) 146–154.
[17] M. Liu, J. Xiao, X.D. Chen, A soft-elastic reactor (SER) inspired from animal upper digestion tract, Chem. Eng. Technol. 41 (2018) 1051–1056.
[18] J. Xiao, C. Zou, M. Liu, G. Zhang, G. Delaplace, R. Jeantet, X.D. Chen, Mixing in a soft-elastic reactor (SER) characterized using an RGB based image analysis method, Chem. Eng. Sci 181 (2018) 272–285.
[19] M. Liu, C. Zou, J. Xiao, X.D. Chen, Soft-elastic bionic reactor, J. Chem. Ind. Eng. (China) 69 (2018) 414–422.
[20] S. Saini, T.M. Wick, Concentric cylinder bioreactor for production of tissue engineered cartilage: effect of seeding density and hydrodynamic loading on construct development, Biotechnol. Progr 19 (2003) 510–521.
[21] M. Cai, X. Zhou, J. Lu, W. Fan, C. Niu, J. Zhou, Enhancing aspergiolide A production from a shear-sensitive and easy-foaming marine-derived filamentous fungus Aspergillus glaucus, by oxygen carrier addition and impeller combination in a bioreactor, Biotechnol. Progr 102 (2011) 3584.
[22] D.J. Lamberto, F.J. Muzzio, P.D. Swanson, A.L Tonkovich, Using time-dependent RPM to enhance mixing in stirred vessels, Chem. Eng. Sci 51 (1996) 733–741.
[23] S. Hashimoto, H. Ito, Y Inoue, Experimental study on geometric structure of isolated mixing region in impeller agitated vessel, Chem. Eng. Sci. 64 (2009) 5173–5181.
[24] M.N. Noui-Mehidi, N. Ohmura, J. Wu, B. Van Nguyen, N. Nishioka, T. Takigawa, Characterisation of isolated mixing regions in a stirred vessel, Int. J. Chem. React. Eng. 6 (2008).
[25] S. Wang, J. Wu, E. Bong, Reduced IMRs in a mixing tank via agitation improvement, Chem. Eng. Res. Des. 91 (2013) 1009–1017.
[26] K. Takahashi, M. Motoda, Chaotic mixing created by object inserted in a vessel agitated by an impeller, Chem. Eng. Res. Des. 87 (2009) 386–390.
[27] T. Nomura, T. Uchida, K Takahashi Takahashi, Enhancement of mixing by unsteady agitation of an impeller in an agitated vessel, J. Chem. Eng. Jpn. 30 (1997) 875–879.
[28] Y. Hirata, T. Dote, T. Yoshioka, Y. Komoda, Y. Inoue, Performance of chaotic mixing caused by reciprocating a disk in a cylindrical vessel, Chem. Eng. Res. Des. 85 (2007) 576–582.
[29] H. Aref, S. Balachandar, Chaotic advection in a Stokes flow, Phys. Fluids 29 (1986) 3515–3521.
[30] W.M. Lu, H.Z. Wu, M.Y. Ju, Effects of baffle design on the liquid mixing in an aerated stirred tank with standard rushton turbine impellers, Chem. Eng. Sci. 52 (1997) 3843–3851.
[31] J. Karcz, M. Cudak, J. Szoplik, Stirring of a liquid in a stirred tank with an eccentrically located impeller, Chem. Eng. Sci. 60 (2005) 2369–2380.
[32] K. Takahashi, Y. Sugo, Y. Takahata, H. Sekine, M. Nakamura, Laminar mixing in stirred tank agitated by an impeller inclined, Int. J. Chem. Eng (2012) 1–10, 2012.
[33] Z. Liu, X. Zheng, D. Liu, Y. Wang, C Tao, Enhancement of liquid–liquid mixing in a mixer-settler by a double rigid-flexible combination impeller, Chem. Eng. Process. 86 (2014) 69–77.
[34] D. Gu, Z. Liu, C. Xu, J. Li, Y Wang, Solid-liquid mixing performance in a stirred tank with a double punched rigid-flexible impeller coupled with a chaotic motor, Chem. Eng. Process. 118 (2017) 37–46.
[35] D. Gu, Z. Liu, Z. Li, C. Xie, Y. Wang, Intensification of chaotic mixing in a stirred tank with a punched rigid-flexible impeller and a chaotic motor, Chem. Eng. Process. 122 (2017) 1–9.
[36] J.P. Zha, S.Y. Zou, J.Y. Hao, X.J. Liu, G. Delaplace, R. Jeantet, D. Dupont, P. Wu, X. D. Chen, J. Xiao, The role of circular folds in mixing intensification in the small intestine: a numerical study, Chem. Eng. Sci. 229 (2021) 1–20.
[37] Y.N. Zhang, P. Wu, R. Jeantet, D. Dupont, G. Delaplace, X.D. Chen, J. Xiao, How motility can enhance mass transfer and absorption in the duodenum: taking the structure of the villi into account, Chem. Eng. Sci. 213 (2020) 1–13.
[38] P. Mavros, Flow visualization in stirred vessels: a review of experimental techniques, Chem. Eng. Res. Des. 79 (2001) 113–127.
[39] G. Ascanio, Mixing time in stirred vessels: a review of experimental techniques, Chin. J. Chem. Eng. 23 (2015) 1065–1076.
[40] G. Delaplace, L. Bouvier, A. Moreau, R. Guérin, J.C. Leuliet, Determination of mixing time by colourimetric diagnosis application to a new mixing system, Exp. Fluids 36 (2004) 437–443.
[41] F. Cabaret, S. Bonnot, L. Fradette, P.A. Tanguy, Mixing time analysis using colorimetric methods and image processing, Ind. Eng. Chem. Res 46 (2007) 5032–5042.
[42] L. Vega-Alvarado, B. Taboada, A. Hidalgo-Millán, G. Ascanio, An image analysis method for the measurement of mixing times in stirred vessels, Chem. Eng. Technol 34 (2011) 859–866.
[43] L. Vega-Alvarado, B. Taboada, A. Hidalgo-Millán, G. Ascanio, On the measurement and scaling of mixing time in orbitally shaken bioreactors, Biochem. Eng. J 82 (2014) 10–21.
[44] G. Rodriguez, W. Weheliye, T. Anderlei, M. Micheletti, M. Yianneskis, A. Ducci, Mixing time and kinetic energy measurements in a shaken cylindrical bioreactor, Chem. Eng. Res. Des 91 (2013) 2084–2097.
[45] J.M. Ottino, The Kinematics of mixing: stretching, chaos, and Transport, 1st edition, Cambridge university press, United Kingdom, 1989, pp. 2–10.
[46] S. Bale, K. Clavin, M. Sathe, A.S. Berrouk, F.C. Knopf, K. Nandakumar, Mixing in oscillating columns: experimental and numerical studies, Chem. Eng. Sci. 168 (2017) 78–89.